Optimal SOC Headroom of Pump Storage Hydropower for Maximizing Joint Revenue from Day-ahead and Real-time Markets Under Regional Transmission Organization Dispatch

Yikui Liu, Bing Huang, Yang Lin, Yonghong Chen, and Lei Wu

***Abstract*—In response to the increasing penetration of volatile and uncertain renewable energy, the regional transmission organizations (RTOs) have been recently focusing on enhancing the models of pump storage hydropower (PSH) plants, which are one of the key flexibility assets in the day-ahead (DA) and real-time (RT) markets, to further boost their flexibility provision potentials. Inspired by the recent research works that explored the potential benefits of excluding PSHs' cost-related terms from the objective functions of the DA market clearing model, this paper completes a rolling RT market scheme that is compatible with the DA market. Then, with the vision that PSHs could be permitted to submit state-of-charge (SOC) headrooms in the DA market and to release them in the RT market, this paper uncovers that PSHs could increase the total revenues from the two markets by optimizing their SOC headrooms, assisted by the proposed tri-level optimal SOC headroom model. Specifically, in the proposed tri-level model, the middle and lower levels respectively mimic the DA and RT scheduling processes of PSHs, and the upper level determines the optimal headrooms to be submitted to the RTO for maximizing the total revenue from the two markets. Numerical case studies quantify the profitability of the optimal SOC headroom submissions as well as the associated financial risks.**

***Index Terms*—Pump storage hydropower, energy market, state-of-charge (SOC), headroom, market revenue, tri-level problem.**

NOMENCLATURE

A. Indices, Sets, and Symbols

$\tau(v)$	An index mapping function that returns hour index corresponding to sub-hour v of real-time (RT) market
$card(\cdot)$	Cardinality of a set
s, $\mathcal{S}$	Index and set of locational marginal price (LMP) scenarios
t, $\mathcal{T}$	Index and set of hours at day-ahead (DA) scheduling level of the proposed tri-level model, i.e., $t \in \mathcal{T} = \{1, 2, \ldots, T\}$ and $T = 24$
v	Index of sub-hour time intervals in RT market
$\mathcal{V}$	Set of sub-hour time intervals at RT scheduling level of the proposed tri-level model, i.e., $\mathcal{V} = \{1, 2, \ldots, V\}$
$\mathcal{V}^{\mathrm{ET}}$	Set of extended time intervals in RT market
$\mathcal{V}^{\mathrm{BD}}$	Set of binding time intervals of all RT markets in a day

B. Parameters

η^{P}, η^{G}	Pumping and generating efficiencies of a PSH
ρ_s	Probability, i.e., weight, of scenario s
Δt	Timespan of one sub-hour time interval at RT scheduling level of the proposed tri-level model
G^{LB}, G^{UB}	Generating power lower and upper bounds of a pump storage hydropower (PSH)
H^{L}, H^{U}	Lower and upper state-of-charge (SOC) headrooms of a PSH
$H^{\mathrm{L,LIM}}$, $H^{\mathrm{U,LIM}}$	Limits of lower and upper SOC headrooms of a PSH
$LMP^{\mathrm{DA}}_{t,s}$	LMP at hour t in scenario s at DA scheduling level of the proposed tri-level model
$LMP^{\mathrm{RT}}_{v,s}$	LMP at sub-hour v in scenario s at RT scheduling level of the proposed tri-level model
$LMP^{\mathrm{RT,FR}}_{v}$	LMP forecasting for extended sub-hour v in RT market
P^{LB}, P^{UB}	Lower and upper bounds of pumping power of a PSH
SOC^{LB}, SOC^{UB}	Lower and upper SOC bounds of a PSH

Manuscript received: February 13, 2023; revised: April 19, 2023; accepted: July 6, 2023. Date of CrossCheck: July 6, 2023. Date of online publication: July 28, 2023.

Y. Liu, Y. Lin, and L. Wu (corresponding author) are with Electrical and Computer Engineering Department, Stevens Institute of Technology, Hoboken, NJ 07030, USA (e-mail: yliu262@stevens.edu; ylin17@stevens.edu; lei.wu@stevens.edu).

B. Huang and Y. Chen are with Midcontinent Independent System Operator, Inc., Carmel, IN 46032, USA (e-mail: BHuang@misoenergy.org; yhen@misoenergy.org).

DOI: 10.35833/MPCE.2023.000087

SOC^{IN}, SOC^{TM} — Initial and terminal SOCs of a PSH

CAP — Capacity of a PSH

C. Continuous Variables

h^{L}, h^{U} — Headrooms on lower and upper SOC bounds of a PSH

p_t^{DA}, g_t^{DA} — Pumping and generating power at hour t in DA market

$p_{t,s}^{\mathrm{DA}}$, $g_{t,s}^{\mathrm{DA}}$ — Pumping and generating power at hour t in scenario s at DA scheduling level of the proposed tri-level model

$p_{v,s}^{\mathrm{RT}}$, $g_{v,s}^{\mathrm{RT}}$ — Pumping and generating power at sub-hour v in scenario s at RT scheduling level of the proposed tri-level model

p_v^{RT}, g_v^{RT} — RT pumping and generating power at sub-hour v of an RT market

soc_t^{DA} — DA SOC at hour t

$soc_{t,s}^{\mathrm{DA}}$ — SOC at hour t in scenario s at DA scheduling level of the proposed tri-level model

$soc_{v,s}^{\mathrm{RT}}$ — SOC at sub-hour v in scenario s at RT scheduling level of the proposed tri-level model

D. Binary Variables

$u_t^{\mathrm{P,DA}}$, $u_t^{\mathrm{G,DA}}$ — Pumping and generating statuses at hour t in DA market

$u_{t,s}^{\mathrm{P,DA}}$, $u_{t,s}^{\mathrm{G,DA}}$ — Pumping and generating statuses at hour t in scenario s at DA scheduling level of the proposed tri-level model

$u_{v,s}^{\mathrm{P,RT}}$, $u_{v,s}^{\mathrm{G,RT}}$ — Pumping and generating statuses at sub-hour v in scenario s at RT scheduling level of the proposed tri-level model

I. Introduction

REGIONAL transmission organizations (RTOs) in the U.S. have witnessed the rapid growth of renewable energy in recent years. Among heterogeneous renewable energy technologies, solar energy and wind energy present the most prominent propositions and manifest a rather faster growth trend. For instance, about half of the demand in California Independent System Operator's (CAISO's) control area is supplied by solar energy during the daytime. As another example, in Midcontinent Independent System Operator (MISO), the total installed capacity of wind energy has exceeded 26 GW with an average hourly wind energy output of 8 GWh, accounting for 12% of the average hourly electric energy output from all resources in 2020 [1]. However, solar energy and wind energy present noticeable variability and uncertainty, which cause critical challenges to system reliability and the great need for system flexibility.

To facilitate deeper integration of renewable energy, it becomes necessary to incent existing units, e.g., combined-cycle gas turbines (CCGTs) and pump storage hydropower (PSH) plants, with fast-response and quick-ramping abilities for providing system flexibility. Enhanced system scheduling platforms and asset dispatching models could help augment the effective utilization of these existing flexibility resources in the system by exploring their full flexibility potential. Indeed, CCGTs and PSHs are among the recent focuses [2]-[4] because: ① they are ideal system flexibility providers; ② their dispatching models are more complicated than ordinary thermal units; and ③ their dispatching models are oversimplified in the current RTO market clearing model, which otherwise could dramatically enhance the effective utilization of their full flexibility potentials.

This paper focuses on PSH plant modeling in the current RTO market clearing practice. For instance, in the MISO market, a PSH can exclusively bid as an ordinary generation source or a price-sensitive load in each time interval of the day-ahead (DA) market, requiring PSHs to pre-determine their pumping and generating plans. Then, MISO optimizes the generating mode using the maximum daily energy constraint. The development of the next-generation market clearing model is the state-of-charge (SOC) based formulation [5], [6], which tracks dynamic SOC levels via SOC evolution, SOC boundary, and dispatchable range constraints. The SOC-based formulation allows the RTO to co-optimize pumping and generating modes of PSHs with other generation and load resources to achieve the highest social welfare. In the academic field, this formulation has become the most fundamental and typical dispatching model [7], [8], and many related delicate variants have been studied [9] - [15]. References [9] and [10] integrate the SOC-based PSH formulation into unit commitment problems under a robust framework and a stochastic framework. References [11] and [12] determine the power generation of a hydro unit while considering the joint effects of water head, water tail, and water discharge. References [14] and [15] put their focus on modeling the reserve provision of PSHs. However, from the perspective of RTO, the balance between model accuracy, computational efficiency, and data availability is always a lingering challenge. Therefore, these SOC-based models are unlikely to be implemented in the near future by RTOs, mainly due to the concern about computational performance. It is worth mentioning that [6] interestingly extends the PSH formulation into a mode transition based PSH operation model, analogous to the configuration based CCGT model, and tests this model with DA market cases of MISO.

Notably, different from traditional generators, SOC constraints of energy-limited PSHs induce new challenges in exactly following energy and reserve instructions of RTO over time. Specifically, SOC limits imply restricted stored energy and spare storage space, which cannot freely support prolonged energy and reserve deployment. Because of this energy-limited characteristic, the SOC headroom model of PSHs in the RTO DA market is explored in [16] and [17], intending to withhold sufficient stored energy and storage for ensuring that reserves of PSHs cleared in the DA market are deliverable in the real-time (RT) markets. On the one hand, SOC headrooms could avoid exhausting PSH capability in the DA stage and be conducive to system security in RT operations. References [16] and [17] discuss the importance of

enforcing SOC headrooms to withhold the capability from the perspective of securely delivering the DA-scheduled reserve in the RT markets. On the other hand, releasing withheld energy and capacity in the RT markets could possibly bring higher total revenues to PSHs from the two markets jointly. This could be achieved by leveraging the locational marginal price (LMP) differences between the two markets to release the SOC headroom of PSHs in RT on request. However, most of the existing research works mainly focus on the system security but rarely analyze the proper headrooms from the angle of PSH profit.

Focusing on the energy markets of RTOs in the U.S., [6] proposes to have PSHs fully optimized by RTOs, by excluding the cost of PSHs from the objective function of the DA market of RTOs. This is motivated by the observation that the flexibility of PSHs has not been fully explored. Indeed, inappropriate bids of PSHs frequently make them miss the opportunity of being cleared and arbitraging in the RT market. Nevertheless, this idea may not be directly extendable to the RT market because its rolling scheme has no or limited look-ahead time window. This motivates [18] to initiate the effort of realizing this idea in the RT market so that the RTOs could achieve the fully optimized utilization of PSHs. In this paper, inspired by [18], we complete the design of a rolling RT market scheme that realizes the idea and is fully compatible with the DA market scheme. Under this market scheme, we envision that the RTOs in the U.S. with similar market structures and policies could allow PSHs to submit the lower and upper SOC headrooms in the DA market on a daily basis and release them in the RT market. We propose a tri-level problem from the perspective of PSH owners to assist them in optimizing the SOC headrooms submitted to the DA markets of RTOs, for achieving the highest total revenues from the two markets.

The contributions of this paper are twofold:

1) Following the innovative DA market scheme [6] of co-optimizing PSHs with other resources by the RTOs while excluding cost-related terms of PSHs from the objective function, we design a corresponding rolling RT market scheme that is compatible with the DA market scheme.

2) Envisioning that the RTOs could allow PSHs to submit two SOC headrooms, a tri-level optimal SOC headroom model is proposed to assist PSHs in optimally determining their SOC headrooms in achieving the highest joint revenue in DA and RT markets.

The rest of the paper is organized as follows. The new role of PSHs in the RTO markets is introduced in Section II. Section III presents the optimizing headroom submissions for PSHs. Numerical case studies are conducted in Section IV, and the conclusions are drawn in Section V. Please note that the views expressed herein do not necessarily represent those of the MISO.

II. New Role of PSHs in RTO Markets

According to the technologies of installed generators, PSHs can be classified into single-speed PSHs and adjustable-speed PSHs. Both types can generate at variable power levels, but the former pumps at a fixed power level, while the latter can adjust the pumping power level within a range. Adjustable-speed PSHs are the focus of this paper. The RTO oversees the DA and RT markets. Referring to the DA bids, it clears the DA market to determine the unit commitment and base power dispatches of the next operation day. During the operation day, the RTO, referring to the RT bids as well as the unit commitment results from the DA market, clears the RT market in a rolling manner to balance power generation and RT demand.

A. DA Market Model of RTO to Optimize PSH Operations

A PSH optimized by the RTO in the DA market can be modeled as in constraints (1). Power dispatchable ranges under generating and pumping modes are formulated as in (1a) and (1b), respectively; constraint (1c) ensures the exclusiveness of the pumping and generating modes; SOC evolution is represented as in (1d); SOC boundaries are enforced by (1e); constraints (1f) and (1g) specify the initial and terminal SOC levels at the beginning and end of the day, respectively.

$$G^{\mathrm{LB}} u_t^{\mathrm{G,DA}} \le g_t^{\mathrm{DA}} \le G^{\mathrm{UB}} u_t^{\mathrm{G,DA}} \quad \forall t \in \mathcal{T} \tag{1a}$$

$$P^{\mathrm{LB}} u_t^{\mathrm{P,DA}} \le p_t^{\mathrm{DA}} \le P^{\mathrm{UB}} u_t^{\mathrm{P,DA}} \quad \forall t \in \mathcal{T} \tag{1b}$$

$$u_t^{\mathrm{G,DA}} + u_t^{\mathrm{P,DA}} \le 1 \quad \forall t \in \mathcal{T} \tag{1c}$$

$$soc_t^{\mathrm{DA}} \cdot CAP = soc_{t-1}^{\mathrm{DA}} \cdot CAP + \eta^{\mathrm{P}} p_t^{\mathrm{DA}} - \frac{1}{\eta^{\mathrm{G}}} g_t^{\mathrm{DA}} \quad \forall t \in \mathcal{T} \tag{1d}$$

$$SOC^{\mathrm{LB}} \le soc_t^{\mathrm{DA}} \le SOC^{\mathrm{UB}} \quad \forall t \in \mathcal{T} \tag{1e}$$

$$soc_0^{\mathrm{DA}} = SOC^{\mathrm{IN}} \tag{1f}$$

$$soc_{\mathrm{T}}^{\mathrm{DA}} = SOC^{\mathrm{TM}} \tag{1g}$$

Based on the above PSH model (1), [6] innovatively proposes to remove the PSH related terms, including power generating and pumping bids, startup costs, and no-load costs, from the objective function of the DA market clearing model, allowing PSHs to be fully optimized by RTOs according to the system needs. Numerical studies with production cases of MISO [6] have shown three encouraging observations: ① although optimized by the RTO instead of designing comprehensive bidding strategies, the DA market revenues of PSHs are likely to be higher than the original setting, i.e., when including the PSH bids in the objective; ② PSHs can be flexibly dispatched according to the system needs instead of following their pre-specified generating and pumping schedules, i.e., generating and pumping schedules optimized by RTOs align with LMP signals; and ③ this enhanced flexibility of PSHs helps reduce operating costs of the entire system. It is worthwhile to mention that the SOC terminal constraint (1g) is introduced to avoid the exhaustive generation of PSHs in the absence of bids, otherwise, the stored energy becomes free and tends to be fully used.

B. RT Market Model of PSHs Compatible with DA Market

With the above change, PSHs will no longer need to submit power generating and pumping bids to RTO in the DA market. To keep the consistency, PSHs shall also be removed from the objective function of the RT market clearing model. Reference [6] does not discuss the corresponding RT market implementation, which in fact could give rise to

a significant challenge. Specifically, different from the DA market in which (1g) could be reasonably enforced to avoid the exhaustive generation of PSHs throughout the entire day, the current RT market implementations have no or limited look-ahead time horizon. This disables directly implementing a counterpart of (1g) in the RT market model when PSHs are removed from the objective function, resulting in potential shortsightedness that PSHs uneconomically exhaust their stored energy quickly while neglecting their potential values in future RT markets.

An intuitive remedy is to enforce the terminal SOCs of PSHs at the end of the look-ahead time horizon equal to their DA scheduled values of the corresponding hours. Although simple and easy to implement, its disadvantage is that the flexibility of PSHs will be severely compromised when the RT market operation condition significantly differs from the DA market, which indeed could make the DA SOC schedules far from optimal for both PSHs and the system in RT.

Another potential option is to extend the look-ahead time horizon to the end of the day so that the DA terminal SOC constraint (1g) can be restored. However, this option could raise data availability and computational issues. The extra computational burden is inevitable as the problem scale increases, raising concerns for RT markets which have strict solution time limits. Moreover, the RT market bids of other resources could be updated with market rolling forward, and only cover a short period of future time instead of the entire day. Thus, RT market bids of other resources in extended time intervals may be unavailable in the current RT market run.

Reference [18] proposes to merely model PSHs in extended time intervals and with hourly time granularity, so that terminal SOC constraints can be enforced while avoiding the above two issues. In the extended time intervals, only PSHs related constraints are added, including SOC evolution equations, SOC boundaries, and power dispatchable ranges. However, without the drive of the system needs, in extended time intervals, PSHs will fall into aimlessness. To this end, [18] further introduces the term (2) into the objective function of each RT market run to evaluate the monetary value of generating and pumping in the extended time intervals via the forecasted RT LMPs.

$$\sum_{v \in \mathcal{V}^{\mathrm{ET}}} LMP_v^{\mathrm{RT,FR}} \cdot (g_v^{\mathrm{RT}} - p_v^{\mathrm{RT}}) \tag{2}$$

C. Optimal Headroom of PSHs Submitted to RTO

In this paper, we consider that besides upper and lower SOC bounds which represent physical limits and remain unchanged for a relatively long period of time, e.g., weeks or months, RTOs allow PSHs to submit SOC headrooms on a daily basis but merely in the DA market. The SOC headrooms are applied on (1e) as in (3). With this shrunken region for SOC changes, the energy awarded to a PSH in the DA market is likely to be either reduced or gathered in only a few hours.

$$SOC^{\mathrm{LB}} \cdot CAP + H^{\mathrm{L}} \le soc_t^{\mathrm{DA}} \le SOC^{\mathrm{UB}} \cdot CAP - H^{\mathrm{U}} \tag{3}$$

The total revenue of a PSH consists of the DA and RT market parts as in (4), where the first term is the DA revenue and the second term is the RT revenue. The RT revenue of a PSH equals the RT dispatch deviations to its DA awards multiplying RT LMPs. For a PSH under the generation mode, the settlement of 5-min RT markets will ask it to buy back less-generated energy or repay it for extra generation at the RT LMP referring to its DA awards. Similarly, under the pumping mode, the PSH will pay for over-pumped energy or be paid for less-pumped energy referring to its DA awards. Since RT markets are in a rolling scheme, only dispatches of the first interval of each run will be implemented and its corresponding LMP will settle the RT market. Thus, $v \in \mathcal{V}^{\mathrm{BD}}$ has a granularity of 5 min. As DA and RT markets have different time granularities, we use $\tau(v)$ to map sub-hour v to the corresponding hour in the DA market.

$$\sum_{t \in \mathcal{T}} LMP_t^{\mathrm{DA}} \cdot (g_t^{\mathrm{DA}} - p_t^{\mathrm{DA}}) + \sum_{v \in \mathcal{V}^{\mathrm{BD}}} LMP_v^{\mathrm{RT}} \cdot [(g_v^{\mathrm{RT}} - p_v^{\mathrm{RT}}) - (g_{\tau(v)}^{\mathrm{DA}} - p_{\tau(v)}^{\mathrm{DA}})]\Delta t \tag{4}$$

When a PSH foresees that the RT LMP will be higher than the DA LMP, it can leverage H^{L} to reserve a certain amount of energy to be released in RT. This allows g_v^{RT} to be larger than $g_{\tau(v)}^{\mathrm{DA}}$ in (4) when LMP_v^{RT} is higher than LMP_t^{DA}, which could bring extra revenues to the PSH. Similarly, when a lower RT LMP is expected, the PSH can reserve its storage via H^{U} for activating pumping in real time. This enlarges the difference between $p_{\tau(v)}^{\mathrm{DA}}$ and p_v^{RT} in (4) and brings extra stored energy. Ideally, if the above two situations happen at peak and valley load hours, the PSH could potentially profit more by arbitraging with the extra energy in real time. It is noteworthy that improper SOC headrooms may reverse the above revenue analysis and make PSHs potentially lose revenues compared with the case without SOC headrooms.

III. Optimizing Headroom Submissions for PSHs

A. Optimal SOC Headroom Model of PSHs

The optimal SOC headroom model of a PSH is formulated as a stochastic tri-level problem (5)-(9), in which the upper-level problem determines the optimal SOC headrooms that would achieve the maximum expected revenue from the DA and RT markets jointly. The objective function (5) is a stochastic reformulation of (4) over a set of market price scenarios, which is constrained by the middle-level (8) and the lower-level (9) optimization problems that respectively mimic the PSH schedule optimized by the RTO in the DA and RT markets. Hereafter, they are referred to as the DA and RT scheduling levels of RTO. This stochastic tri-level model will be built and solved by the PSH to optimize its SOC headrooms submitted to the DA market of RTO. It is noted that (5) calculates the revenue of PSHs, instead of their net profits which can be computed by subtracting the startup costs of PSHs. Following the objective of the DA market of RTO [6], startup costs are not included in the tri-level problem (5)-(9) because they are usually negligibly small [6]. In addition, according to the current market practice, if the revenue of a PSH cannot cover its total cost, including the start-

up cost, it will be compensated with extra uplift payments.

$$\max_{h^{\mathrm{L}},h^{\mathrm{U}}} \sum_{s\in\mathcal{S}}\rho_s\left\{\sum_{t\in\mathcal{T}} LMP_{t,s}^{\mathrm{DA}}\cdot(g_{t,s}^{\mathrm{DA}}-p_{t,s}^{\mathrm{DA}})+ \sum_{v\in\mathcal{V}} LMP_{v,s}^{\mathrm{RT}}\cdot[(g_{v,s}^{\mathrm{RT}}-p_{v,s}^{\mathrm{RT}})-(g_{\tau(v),s}^{\mathrm{DA}}-p_{\tau(v),s}^{\mathrm{DA}})]\Delta t\right\} \tag{5}$$

$$0\le h^{\mathrm{L}}\le H^{\mathrm{L,LIM}} \tag{6}$$

$$0\le h^{\mathrm{U}}\le H^{\mathrm{U,LIM}} \tag{7}$$

1) DA Scheduling Level of RTO

$$g_{t,s}^{\mathrm{DA}},p_{t,s}^{\mathrm{DA}},u_{t,s}^{\mathrm{G,DA}},u_{t,s}^{\mathrm{P,DA}}= \underset{g_{t,s}^{\mathrm{DA}},p_{t,s}^{\mathrm{DA}},u_{t,s}^{\mathrm{G,DA}},u_{t,s}^{\mathrm{P,DA}}}{\arg\max} \sum_{t\in\mathcal{T}} LMP_{t,s}^{\mathrm{DA}}\cdot(g_{t,s}^{\mathrm{DA}}-p_{t,s}^{\mathrm{DA}}) \quad \forall s\in\mathcal{S} \tag{8a}$$

$$G^{\mathrm{LB}}u_{t,s}^{\mathrm{G,DA}}\le g_{t,s}^{\mathrm{DA}}\le G^{\mathrm{UB}}u_{t,s}^{\mathrm{G,DA}} \quad \forall t\in\mathcal{T} \tag{8b}$$

$$P^{\mathrm{LB}}u_{t,s}^{\mathrm{P,DA}}\le p_{t,s}^{\mathrm{DA}}\le P^{\mathrm{UB}}u_{t,s}^{\mathrm{P,DA}} \quad \forall t\in\mathcal{T} \tag{8c}$$

$$u_{t,s}^{\mathrm{G,DA}}+u_{t,s}^{\mathrm{P,DA}}\le 1 \quad \forall t\in\mathcal{T} \tag{8d}$$

$$soc_{t,s}^{\mathrm{DA}}\cdot CAP=soc_{t-1,s}^{\mathrm{DA}}\cdot CAP+\eta^{\mathrm{P}}p_{t,s}^{\mathrm{DA}}-\frac{1}{\eta^{\mathrm{G}}}g_{t,s}^{\mathrm{DA}} \quad \forall t\in\mathcal{T} \tag{8e}$$

$$SOC^{\mathrm{LB}}+\frac{h^{\mathrm{L}}}{CAP}\le soc_{t,s}^{\mathrm{DA}}\le SOC^{\mathrm{UB}}-\frac{h^{\mathrm{U}}}{CAP} \quad \forall t\in\mathcal{T} \tag{8f}$$

$$soc_{0,s}^{\mathrm{DA}}=SOC^{\mathrm{IN}} \tag{8g}$$

$$soc_{t,s}^{\mathrm{DA}}=SOC^{\mathrm{TM}} \tag{8h}$$

2) RT Scheduling Level of RTO

$$g_{v,s}^{\mathrm{RT}},p_{v,s}^{\mathrm{RT}},u_{v,s}^{\mathrm{G,RT}},u_{v,s}^{\mathrm{P,RT}}= \underset{g_{v,s}^{\mathrm{RT}},p_{v,s}^{\mathrm{RT}},u_{v,s}^{\mathrm{G,RT}},u_{v,s}^{\mathrm{P,RT}}}{\arg\max} \sum_{v\in\mathcal{V}} LMP_{v,s}^{\mathrm{RT}}\cdot(g_{v,s}^{\mathrm{RT}}-p_{v,s}^{\mathrm{RT}})\Delta t \quad \forall s\in\mathcal{S} \tag{9a}$$

$$G^{\mathrm{LB}}u_{v,s}^{\mathrm{G,RT}}\le g_{v,s}^{\mathrm{RT}}\le G^{\mathrm{UB}}u_{v,s}^{\mathrm{G,RT}} \quad \forall v\in\mathcal{V} \tag{9b}$$

$$P^{\mathrm{LB}}u_{v,s}^{\mathrm{P,RT}}\le p_{v,s}^{\mathrm{RT}}\le P^{\mathrm{UB}}u_{v,s}^{\mathrm{P,RT}} \quad \forall v\in\mathcal{V} \tag{9c}$$

$$u_{v,s}^{\mathrm{G,RT}}+u_{v,s}^{\mathrm{P,RT}}\le 1 \quad \forall v\in\mathcal{V} \tag{9d}$$

$$\begin{cases} u_{v,s}^{\mathrm{G,RT}}\ge u_{\tau(v),s}^{\mathrm{G,DA}} \\ u_{v,s}^{\mathrm{P,RT}}\ge u_{\tau(v),s}^{\mathrm{P,DA}} \end{cases} \quad \forall v\in\mathcal{V} \tag{9e}$$

$$soc_{v,s}^{\mathrm{RT}}\cdot CAP=soc_{v-1,s}^{\mathrm{RT}}\cdot CAP+\eta^{\mathrm{P}}p_{v,s}^{\mathrm{RT}}\Delta t-\frac{1}{\eta^{\mathrm{G}}}g_{v,s}^{\mathrm{RT}}\Delta t \quad \forall v\in\mathcal{V} \tag{9f}$$

$$SOC^{\mathrm{LB}}\le soc_{v,s}^{\mathrm{RT}}\le SOC^{\mathrm{UB}} \quad \forall v\in\mathcal{V} \tag{9g}$$

$$soc_{0,s}^{\mathrm{RT}}=SOC^{\mathrm{IN}} \tag{9h}$$

$$soc_{v,s}^{\mathrm{RT}}=SOC^{\mathrm{TM}} \tag{9i}$$

As market participants, PSHs do not have direct access to system network data and bid information of other assets before market clearing, although some RTOs will reveal bid information after a period of confidentiality. Thus, it is not practically feasible for the PSH to reproduce the energy market model of RTO. Referring [19], it can be derived from Karush-Kuhn-Tucker (KKT) conditions that optimal dispatches from the profit maximization problem of a unit with given LMPs after the market clearing shall be consistent with the optimal schedules determined by RTOs via a convex market clearing model. To this end, we design (8) and (9) that maximize the PSH revenue referring to the corresponding LMPs to approximately mimic the PSH schedule of RTO in the DA and RT markets [19]. This is illustrated in Fig. 1. It is worthwhile to emphasize that (8) and (9) indeed mimic how the PSH will be scheduled by the RTO according to system needs (which shall be consistent with LMP profiles), rather than the model's self-responding against LMPs. Therefore, (8) and (9) adopt the typical dispatching formulation that is consistent with the market clearing model (1) of RTO. We also assume that the impact of the PSH headrooms on LMPs is limited. It is usually valid when the capacity of PSHs is relatively insignificant compared with the total generation capacity of the system. DA LMPs before and after including PSHs headrooms in the DA market clearing model are quantitively compared in the case study to verify that this assumption is held in our simulation setup.

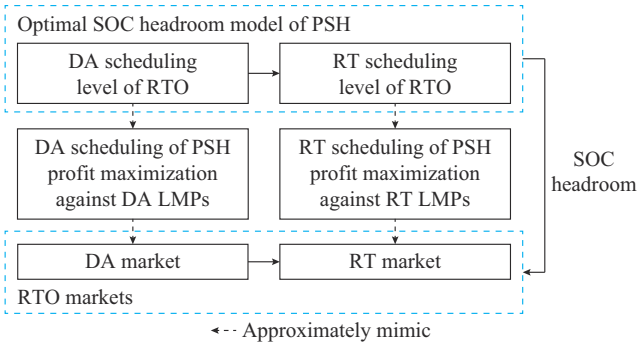

Fig. 1. Relationship between DA and RT scheduling level of PSH and RTO market.

The remaining issue is that actual LMPs remain unknown before the DA and RT markets are settled. To this end, we adopt simulated LMP scenarios, rendering a stochastic tri-level formulation of the optimal SOC headroom model. In this stochastic tri-level model, the upper-level variables h^{L} and h^{U} are scenario-independent. With each LMP scenario s that contains a DA LMP scenario and a corresponding RT LMP scenario, a copy of the DA and RT scheduling levels is built to mimic the corresponding scenario-dependent unit commitment and dispatch schedules optimized by the RTO. Solutions to those dispatch variables, i.e., $g_{t,s}^{\mathrm{DA}}$, $p_{t,s}^{\mathrm{DA}}$, $g_{v,s}^{\mathrm{RT}}$, and $p_{v,s}^{\mathrm{RT}}$, will impact the objective function (5) with weight ρ_s, i.e., the probability of scenario s, which satisfies $\sum_{s\in\mathcal{S}}\rho_s=1$. Reference [20] proposes some practical LMP forecasting and scenario generation methods that properly fit the LMP simulation need of the proposed model. Thus, LMP forecasting and scenario generation methods will not be elaborated as they are not the focus of this paper. Alternatively, the impact of scenarios on the performance of the proposed tri-level model will be quantitatively assessed via case studies in Section IV.

In the upper level, the boundary constraints (6) and (7) restrict the ranges of SOC headrooms. The DA and RT scheduling levels of RTO consist of multiple parallel sub-problems, each of which represents a scenario of LMPs as indicated by subscript s of the variables. At the DA scheduling level of RTO (8), constraints (8b)-(8e) and (8g)-(8h) are respectively the stochastic reformulation of constraints (1a)-

(1d) and (1f)-(1g), and constraint (8f) with the upper-level variables h^{L} and h^{U} is the stochastic reformulation of (3). At the RT scheduling level of RTO (9), constraints (9b)-(9d) and (9h)-(9i) have the same meaning as constraints (1a)-(1c) and (1f)-(1g), respectively. Constraint (9e) connects the DA and RT scheduling levels of RTO, describing that the RTO would keep the RT scheduling of PSH to be consistent with the DA market, which means they can be re-committed but not de-committed. This setting refers to the current practice of MISO that most PSHs do not participate in RT commitment, namely, they comply with DA commitment as much as possible. Constraint (9f) represents the SOC evolution in real time, while different from the DA scheduling level model, the timespan of each time interval is explicitly written out since it is less than an hour, i.e., $\Delta t < 1$. In addition, different from the SOC boundary limits at the DA scheduling level, the headrooms h^{L} and h^{U} are removed from constraint (9g), meaning the stored energy and storage withheld in the DA market can be released in the RT scheduling.

Besides the hourly DA market and the 5-min RT market, an RT commitment that runs in between, e.g., 15-min intervals, can recommit offline fast-startup units such as PSHs. Indeed, the RT scheduling level (9) combines the 5-min RT market and the RT commitment. To this end, we could set $\Delta t = 0.25$, i.e., 15 min, and $card(\mathcal{V}) = 96$, namely $\mathcal{V} = 96$. Correspondingly, $LMP_{v,s}^{\mathrm{RT}}$ of each 15-min v can be set as the average of three underneath 5-min LMPs.

B. Solution Methodology

It is direct to observe that, in the proposed tri-level problem (5)-(9), the upper level only contains two continuous variables h^{L} and h^{U} together with their boundary constraints, while the other two levels are mixed-integer linear programming (MILP) problems of moderate size that can be efficiently solved via commercial solvers. This neat structure of the upper-level problem indeed makes the searching of h^{L} and h^{U} rather straightforward. With this, instead of seeking complicated mathematical methods to equivalently reformulate the tri-level problem (5)-(9) into a single-level optimization model for the solution, it is possible to use a brute-force search for discovering a near-optimal solution. Specifically, we could use multiple points to discretize the entire SOC headroom range, calculate objective values (5) for individual discretized points, and select the one with the best value as the final solution. However, a higher discretization granularity undoubtedly results in a heavier computational burden. Indeed, whenever the discretization granularity is doubled, the points that need to be evaluated will be quadrupled. A practical method could be to first locate a small range with coarse granularity, and then refine the solution within the identified range using a finer granularity.

Alternatively, we use the differential evolution (DE) algorithm [21], which is an evolutionary method that can effectively solve this tri-level model through an iterative process. Specifically, in each iteration, DE is employed to update h^{L} and h^{U} according to the results of DA and RT scheduling levels of RTO in the previous iteration, and the DA and RT scheduling levels of RTO (8) and (9) are solved sequentially as MILP problems based on the updated h^{L} and h^{U} values.

Similar to other evolutionary methods, first, a population of N points are randomly generated to initialize $h_0^{\mathrm{L}n}$ and $h_0^{\mathrm{U}n}$ for $n = 1, 2, \ldots, N$. In each DE iteration k ($k = 1, 2, \ldots, K$), the DE algorithm applies strategies such as rescaling and crossing, and adds additional randomness on each point n ($n = 1, 2, \ldots, N$) to generate new tentative points. Then, with the tentative points, the DA scheduling level of RTO is solved and the solutions to $u_{t,s}^{\mathrm{G,DA}}$ and $u_{t,s}^{\mathrm{P,DA}}$ are passed to the RT scheduling level of RTO that will be solved next. The results from the two levels are used to assess the objective function (5) of individual tentative points. For each point n, if its objective value is smaller than that of the corresponding tentative point, point n will be updated with its corresponding tentative point; otherwise, point n will keep unchanged. After all points have been evaluated, the DE algorithm enters the next iteration. This iterative process terminates after the number of interactions reaches the pre-specified threshold K, and the point with the highest objective value is the final solution. It is worth mentioning that during the iterative process, for an infeasible point, its corresponding objective value is set as negative infinity, and its values h^{L} and h^{U} violating (6) and/or (7) are fixed to the closest boundary. The flowchart of the DE-based solution algorithm is shown in Fig. 2. The further explanation and the pseudocode are provided in the Appendix A.

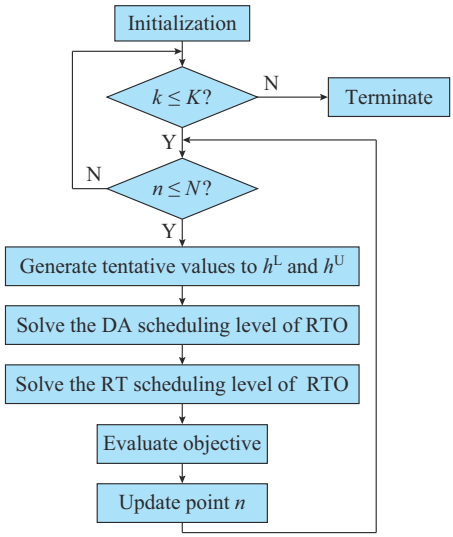

Fig. 2. Flowchart of DE-based solution algorithm.

In fact, with a proper K, all generated points are expected to converge. In other words, all the points will finally produce identical or close-enough solutions. Although non-convergence may not necessarily compromise the discovery of a final solution, convergence usually implies final solutions of higher quality. However, an excessively large K could introduce unnecessary computation, because, after a certain number of iterations, the best objective will only improve marginally. Thus, a comprehensive K setting combined with an appropriate N value could usually bring good-enough performance [21].

IV. Case Studies

A. Market Platform Implementation and Test System Setup

1) Implementation of DA and RT Markets

The effectiveness of the SOC headrooms calculated by the proposed optimal SOC headroom model in Section III will be evaluated via the total revenue of PSHs. We implement a platform with DA and RT market clearing functionalities to calculate the total revenue of PSHs from the two markets. The total revenue throughout a day is calculated as in (4).

1) DA market: the DA market has a time horizon of 24 hours, i.e., $card(\mathcal{T})=24$. The PSH model in the DA market includes constraints (1a)-(1d), (1f)-(1g), and (3). In (3), SOC headrooms H^{L} and H^{U} come from the proposed optimal SOC headroom model (5)-(9).

2) RT market: referring to the RT market timeline of New York Independent System Operator (NYISO) [22], we implement a modified RT market scheme as shown in Fig. 3. Each RT market run covers a 5-min binding time interval, a look-ahead time interval of varying time lengths, and an extended time interval.

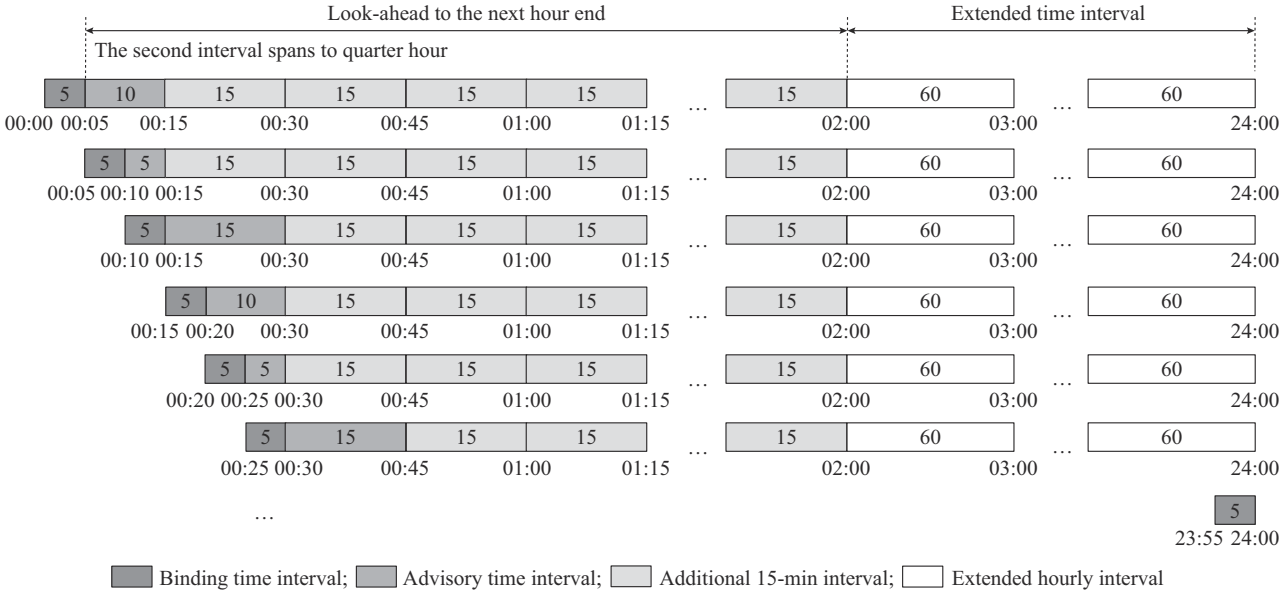

Fig. 3. RT market timeline implementation.

The binding time interval spans the first 5 min. This interval calculates LMPs and energy awards and rolls forward 5 min at each RT market run. Energy awards are released to units, including PSHs, for implementation.

The look-ahead time interval spans till the end of the next hour. It includes one advisory time interval of a varying time length that is right after the binding time interval, followed by additional 15-min intervals to cover the end of the next hour. The timespan of the advisory time interval is determined by the remaining time to the next quarter-hour, namely the 0^{th}, 15^{th}, 30^{th}, and 45^{th} min of an hour. Thus, in each RT market run, depending on its starting time, the time length of the advisory time interval changes cyclically among 5, 10, and 15 min, and the number of additional 15-min intervals varies from 3 to 7.

The extended time intervals with a one-hour step span till the end of the day, and they are used to extend the look-ahead time intreval and are especially valuable for PSHs to facilitate their SOC scheduling throughout the day.

In this scheme, the objective functions of the DA and RT markets of RTO are to maximize social welfare [6], [18] while excluding PSH bids. Unit commitments of thermal units are fixed from the DA to RT. PSHs can be re-committed but not decommitted in RT, and their binding recommitment will be determined every quarter by RT market running on the 0^{th}, 15^{th}, 30^{th}, and 45^{th} min of an hour that contains a 10-min advisory time interval. This implementation indeed incorporates the 15-min RT commitment into the 5-min RT scheduling [23].

2) Test System Setup

We use a modified IEEE 118-bus system with 2 PSHs as the test system. The two PSHs share the same physical parameters, but are on different buses, i.e., buses 46 and 60. The capacities of the two PSHs are 100 MWh. For both PSHs, we set $SOC^{\mathrm{LB}}=20\%$ (20 MWh), $SOC^{\mathrm{UB}}=100\%$ (100 MWh), and $SOC^{\mathrm{TM}}=SOC^{\mathrm{IN}}=50\%$ (50 MWh). Lower and upper power bounds of pumping and generating modes are set to be 5 MW and 20 MW, respectively. Pumping and generating efficiencies η^{P} and η^{G} are set to be 0.9. $H^{\mathrm{L,UB}}$ and $H^{\mathrm{U,UB}}$ are not explicitly set. However, to accommodate $SOC^{\mathrm{TM}}=50\%$ (50 MWh), h^{L} and h^{U} are implicitly restricted within [0, 30]MWh and [0, 50]MWh, respectively. The optimal SOC headroom model and the market platform are implemented in MATLAB. The middle and lower levels of the optimal SOC headroom model and the two markets are MILP and linear programming problems, which are solved by Gurobi 9.0.1. We adopt the default settings of Gurobi and the mixed interger programming (MIP) gap is set to be 0%. All numerical simulations are executed on a PC with an Intel(R) Core(TM) i7-4790 CPU @ 3.60 GHz and 16 GB RAM.

The detailed test data and MATLAB code can be found in [22].

Two cases are studied: ① the non-headroom case in which PSHs do not submit SOC headrooms in the DA market, i.e., the current practice, and the corresponding revenue of PSHs is referred to as non-headroom case revenue; and ② the headroom case in which PSHs submit SOC headrooms derived by the proposed optimal SOC headroom model (5)-(9) in the DA market, and the corresponding revenue of PSHs is referred to as headroom case revenue. The revenue of PSHs calculated via the DA and RT markets in Section IV is referred to as the actual revenue, while the objective value (5) of the proposed optimal SOC headroom model is referred to as the approximated revenue. The solving time of the DA market is around 6 s, and that of a single RT market is 9.8 s on average. The solving time of the optimal SOC headroom model is about 1600 s.

B. Rationality of SOC Headrooms Under Ideal Setup

Intuitively, the quality of LMP scenarios used in the optimal SOC headroom model (5)-(9) could noticeably impact the financial consequence of its produced SOC headroom submissions in the markets. To justify the rationality of submitting SOC headrooms in the DA market while avoiding mixing the impacts of quality of LMP scenarios, we first adopt an ideal setup to illustrate the potential of SOC headrooms in increasing PSH revenues.

Specifically, in the ideal setup, we consider that DA and RT market LMPs of the non-headroom case are available, which can be directly used in the optimal SOC headroom model as the only scenario. These LMPs are obtained by running the DA and RT markets of RTO with the two PSHs. The idea is that the limited capacities of the two PSHs would inconspicuously influence the LMPs. In other words, the LMPs yielded by the non-headroom case shall be rather close to those in the headroom case. Thus, this ideal setup could possibly characterize the best SOC headroom withhold decisions, leading to the maximum potential revenues.

Based on the original hourly load levels of the IEEE 118-bus system, we generate five DA hourly load profiles by rescaling peak loads and introducing fluctuations to simulate five market days. Using the same strategies and applying interpolation between hourly load values, we further create the corresponding RT load profiles that deviate from the DA ones with typical patterns as shown in Table I, which represent potential deviations between the DA and RT load forecasts in practice. Correspondingly, LMPs deviate along with the load profiles and their trends are also shown in Table I. Taking day 2 in Table I as an example, at off-peak hours of this day, the load level and LMP in the RT market are lower than those in the DA market. During peak hours of this day, the load level and LMP in the RT market are higher than those in the DA market.

For each of the five market days, the optimal SOC headroom model is first solved to determine the optimal SOC headrooms. The DA market is then cleared with these derived SOC headrooms. Finally, the RT markets are cleared sequentially, and the total revenue is calculated. The SOC headrooms for the five market days are reported in Table II. SOC headrooms of the two PSHs are generally close because the LMPs at the connection buses of PSHs are close, while SOC headrooms among the 5 days are noticeably different because of different RT load deviation patterns as shown in Table I.

TABLE I
LOAD AND LMP DEVIATION PATTERNS OF RT MARKET TO DA MARKET

Day	Off-peak hours		Peak hours	
	Load level	LMP	Load level	LMP
1	Close RT load	Close RT LMP	Close RT load	Close RT LMP
2	Lower RT load	Lower RT LMP	Higher RT load	Higher RT LMP
3	Lower RT load	Lower RT LMP	Lower RT load	Lower RT LMP
4	Higher RT load	Higher RT LMP	Higher RT load	Higher RT LMP
5	Higher RT load	Higher RT LMP	Lower RT load	Lower RT LMP

Note: off-peak hours denote hours 1-6 and 19-24, when PSHs are likely to pump; and peak hours denote hours 12-18, when PSHs are likely to generate.

TABLE II
OPTIMAL SOC HEADROOMS OF TWO PSHS

Day	PSH 1		PSH 2	
	H^{L} (MWh)	H^{U} (MWh)	H^{L} (MWh)	H^{U} (MWh)
1	9.60	2.21	11.17	0.00
2	28.03	44.47	25.32	49.96
3	0.00	0.00	0.00	0.00
4	27.70	27.76	28.40	27.78
5	0.00	0.00	0.00	0.00

Days 2 and 5 represent two extreme cases with the largest and smallest differences between peak and off-peak hours. On day 2, a higher load level at peak hours induces larger LMPs, while a lower load level at off-peak hours causes smaller LMPs. These together boost the arbitrage potential between the DA and RT markets, leading to large SOC headrooms. In this case, the headrooms of PSH 2 shrink its SOC range in the DA market to [45.32%, 50.04%] ([45.32, 50.04] MWh). Day 5 describes the opposite situation of day 2. When PSHs anticipate that LMPs of off-peak hours in RT could be too high to pump and LMPs of peak hours could be too low to generate, they will become more active in the DA market.

Days 1, 3, and 4 are in between these two extreme cases. Because LMPs of day 1 in the two markets are close, PSHs lack arbitrage opportunities, resulting in limited SOC headrooms. The RT load deviation patterns against the DA on day 3 and day 4 are in opposite directions, causing LMPs to change in opposite directions. The former has lower LMPs at off-peak and peak hours in real time, while the latter has higher ones. Thus, day 3 and day 4 have completely different SOC headrooms, which is a result of the interaction between H^{L} and H^{U}. Specifically, on day 3, if a non-zero H^{U} is applied, it can help PSHs avoid pumping at relatively higher prices in DA, but will also limit the available cycling energy throughout the day and reduce the energy generated

at the peak hours in the DA market. After removing H^{U} in RT, compared with DA, additional energy will be generated at the peak hours, which, will be accounted with lower RT LMPs. By contrast, although the non-zero H^{L} and H^{U} on day 4 will similarly reduce the DA cycling energy, since the additional energy generation in RT will be accounted for with higher RT LMPs, the SOC headrooms would finally boost PSH profit.

Revenues of days 1, 2, and 4 in the non-headroom and headroom cases are further compared in Table III. Day 3 and day 5 are not listed because of their zero SOC headrooms, i. e., their revenues in the non-headroom and headroom cases are the same. In all three listed days, both PSHs more or less achieve extra revenues. For the non-headroom case, in all three days, most revenues come from the DA market. Indeed, the revenue from the RT market, calculated as the second term of (4), could be negative. By contrast, with the headroom case, PSHs start making dramatically more revenue in the RT market. It is not surprising that revenues from the DA market decline to a certain extent because (1e) is replaced by (3) in the non-headroom case. In fact, part of the reduced revenue is realized in the RT market, and potentially with higher gains. An extreme example is day 2, in which the PSHs are not awarded any energy in the DA market because of their large SOC headrooms, but they receive much higher revenues in the RT market. In summary, these studies show that proper SOC headrooms yielded by the proposed optimal SOC headroom model can achieve higher revenues for PSHs.

TABLE III
COMPARISON OF NON-HEADROOM AND HEADROOM CASES

Day	PSH	Revenue of non-headroom case ($)			Revenue of headroom case ($)			
		DA	RT	Total	DA	RT	Total	Increment
1	1	1332.71	5.58	1338.29	1179.65	164.19	1343.85	+5.56
	2	1350.40	–3.45	1346.95	1208.17	147.79	1355.97	+9.02
2	1	1352.85	9.61	1362.46	0.00	2244.07	2244.07	+881.61
	2	1413.38	8.41	1421.79	0.00	2175.80	2175.80	+754.01
4	1	1359.11	1.19	1360.31	426.18	1017.28	1443.47	+83.16
	2	1375.81	–3.41	1372.39	430.51	1007.41	1437.92	+65.53

Note: "increment" indicates the difference to the revenue of non-headroom case.

Finally, Fig. 4 shows the DA LMPs of PSH 1 with and without headrooms, which highly overlap with each other with negligible deviations.

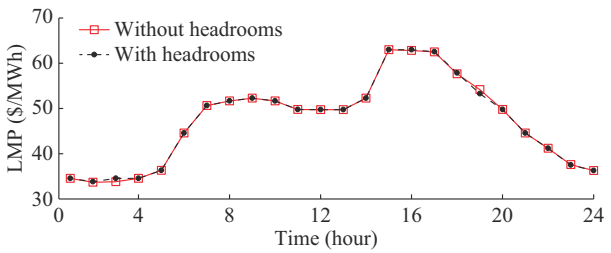

Fig. 4. DA LMPs of PSH 1 with and without headrooms.

The largest deviation is 0.91 $/MWh or 1.67%, occurring at hour 19, while the two LMP profiles are identical in 17 out of 24 hours. This result clearly shows that the assumption of the limited impacts of PSH headrooms on LMPs is valid in this test system.

C. Performance of Proposed Optimal SOC Headroom Model Under Practical Setup

In this subsection, the profitability of the SOC headrooms is further evaluated under a practical setup. Focusing on day 2 and day 4, we assess the impacts of LMP scenario quality on the SOC headrooms and revenues by adding normally distributed random deviations to the DA and RT LMPs of the non-headroom case for mimicking LMP forecasting errors. Four maximum forecasting error levels are considered, including ±5%, ±10%, ±15%, and ±20%. The value of the LMP forecasting error is normally distributed. The normal distribution has zero mean, and its standard deviation is set as 1/3 of the maximum forecasting error multiplying the actual value, i.e., the three-sigma rule of thumb. For each market day and each level of the maximum forecasting error, 30 scenarios are generated. The SOC headrooms and revenues of PSH 1 and PSH 2 on day 2 are shown in Table IV.

TABLE IV
SOC HEADROOMS AND REVENUES OF PSH 1 AND PSH 2 ON DAY 2

The maximum forecasting error (%)	PSH	H^{L} (MWh)	H^{U} (MWh)	Revenue of headroom case ($)			
				DA	RT	Total	Increment
±5	1	25.29	46.11	0	2244.07	2244.07	+881.61
	2	27.77	45.01	0	2175.80	2175.80	+762.42
±10	1	25.33	45.96	0	2244.07	2244.07	+881.61
	2	24.52	47.24	0	2175.80	2175.80	+762.42
±15	1	24.61	47.80	0	2244.07	2244.07	+881.61
	2	27.57	44.78	0	2175.80	2175.80	+762.42
±20	1	27.29	45.11	0	2243.86	2243.86	+881.40
	2	11.58	49.90	360.74	1362.27	1723.01	+350.62

Note: "increment" indicates the difference to the revenue of non-headroom case.

On day 2, except for the maximum forecasting error of ±20%, the final profitability of the two PSHs remains the same as the one calculated under the ideal setup in Section IV-B. This is mainly caused by the close SOC headroom values submitted to the DA market as well as their similar effect in inactivating PSHs in the DA market. We take H^{L} = 25.29 MWh and H^{U} = 46.11 MWh of PSH 1 as an example, which makes the actual dispatchable SOC range in the DA market become 45.29% to 53.89% ([45.29, 53.89]MWh). Considering the pumping and generating efficiencies of 0.9 and power lower bound of 5 MW, the SOC change caused by each hourly pumping and generating actions will be at least +4.5%/–5.55% (+4.5 MWh/–5.55 MWh). However, with the initial SOC of 50% (50 MWh), the SOC range of [45.29%, 53.89%] ([45.29, 53.89]MWh) leaves no room for pumping or generating action at any hour, making the PSH completely inactive in the DA market. Another example is H^{L} = 27.77 MWh and H^{U} = 45.01 MWh, which makes the

corresponding actual dispatchable SOC range in the DA market become [47.77%, 54.99%] ([47.77, 54.99]MWh). This range seems to be able to support one hourly pumping action with the minimum pumping level, changing SOC to 54.5% (54.5 MWh). However, if this action is taken, the PSH can no longer satisfy (1g), i.e., bringing SOC^{TM} back to 50%. When the maximum forecasting error is raised to ±20%, with the generated scenarios, PSH 2 makes a different decision on the headrooms, leading to a different revenue.

The SOC headrooms and revenues of the two PSHs on day 4 are shown in Table V, showing that the SOC headrooms are sensitive to the maximum forecasting errors. In other words, LMP scenarios with different forecasting qualities could lead to noticeably different headrooms and consequently varying total revenues. The results of day 4 show that the SOC headrooms yielded by a higher LMP forecasting accuracy could lead to higher revenue. Indeed, for the maximum forecasting error of ±20%, PSH 1 even loses revenue compared with the non-headroom case. It indicates that submitting SOC headrooms bears certain financial risks with potential revenue loss against the non-headroom case, especially when the LMP forecasting qualities are low.

TABLE V
SOC HEADROOMS AND REVENUES OF TWO PSHS ON DAY 4

The maximum forecasting error (%)	PSH	H^{L} (MWh)	H^{U} (MWh)	Revenue of headroom case ($)			
				DA	RT	Total	Increment
±5	1	28.93	13.95	681.93	711.70	1393.63	+33.32
	2	29.47	31.98	351.71	1148.52	1500.23	+127.84
±10	1	29.03	27.59	429.44	1014.23	1443.68	+83.37
	2	29.62	27.78	430.49	1007.42	1437.92	+65.53
±15	1	29.38	13.94	679.62	721.85	1401.47	+41.16
	2	21.36	13.86	832.36	564.31	1396.67	+24.28
±20	1	11.97	13.98	973.15	371.16	1344.31	−16.00
	2	12.05	32.06	649.98	747.07	1397.05	+24.66

Note: "increment" indicates the difference to the revenue of non-headroom case.

Intuitively, the approximated revenue could deviate from the actual revenue, because of the inaccuracy of the LMP forecasts and the generated scenarios, and the simplified modeling of the actual market operation. Therefore, the given optimal headrooms from the optimal SOC headroom model may not lead to the best actual revenue. The negative increment of −16 dollars shown in Table V is one such example that the optimal SOC headrooms could even reduce the total revenue. To this end, in the next subsection, the ability of the proposed optimal SOC headroom model in approximating the actual revenue will be further evaluated.

D. Approximation Ability of Proposed Optimal SOC Headroom Model

The ability of the proposed optimal SOC headroom model in mimicking the actual markets is further evaluated by comparing the approximated revenue, i.e., the objective function (5) and the corresponding actual headroom case revenue, i.e., revenue calculated via (4) using actual LMPs from the DA and RT market simulations. Obviously, the smaller the difference between the two, the better the approximation ability of the proposed optimal SOC headroom model.

The approximated revenues and the actual revenues of the 3 market days, i.e., days 1, 2, and 4, under the ideal setup are compared in Table VI. The differences between the approximated revenues and the corresponding actual revenues are shown in parentheses in percentages. The comparisons verify the strong simulation ability of the proposed model. In addition, the difference between approximated and actual revenues of the DA market is usually smaller than that of the RT market, indicating that the simulation of the DA market is usually more accurate than the RT market. This is because, in the optimal SOC headroom model, Δt is set to be 15 min to simulate the RT recommitment of PSHs. However, this is incompatible with the 5-min based RT LMPs. To address the incompatibility, the average of three consecutive 5-min LMPs is taken as the 15-min LMP at the RT scheduling level. This adjustment inevitably introduces extra errors. In addition, different from the single run of the DA market, the RT markets are cleared via a rolling manner that could further complicate the simulation accuracy and accumulate approximation errors.

TABLE VI
COMPARISON OF APPROXIMATED AND ACTUAL REVENUES

Day	Revenue of optimal SOC headroom model ($)		Revenue of headroom case ($)	
	PSH 1	PSH 2	PSH 1	PSH 2
1	1391.88 (3.57%)	1410.78 (4.04%)	1343.85	1355.97
2	2250.00 (0.26%)	2181.74 (0.27%)	2244.07	2175.80
4	1519.40 (5.26%)	1549.82 (7.78%)	1443.47	1437.92

The approximated revenue erros under the practical setup are further compared in Fig. 5. Not surprisingly, approximated revenue errors increase with the increase in the maximum forecasting error. Indeed, the increase of the approximated revenue errors in certain cases, e.g., PSH 2 from ±15% to ±20%, is rather significant, emphasizing the importance of the LMP forecasting accuracy to the proposed optimal SOC headroom model.

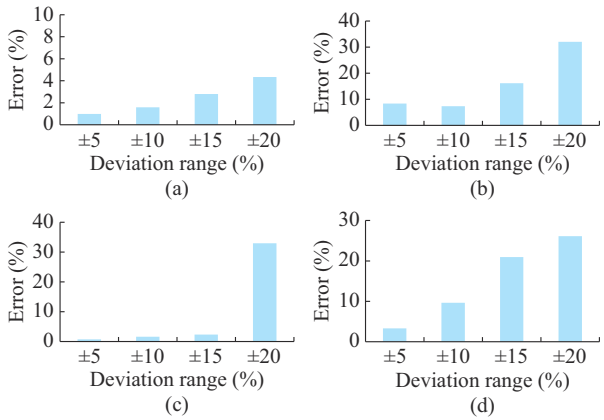

Fig. 5. Approximated revenue errors under practical setup. (a) PSH 1 on day 2. (b) PSH 1 on day 4. (c) PSH 2 on day 2. (d) PSH 2 on day 4.

Moreover, the approximated revenue error could vary significantly on different market days. For PSH 1, the approximated revenue error on day 4 is 6.5 times that on day 2 on average. The high approximated revenue error of PSH 2 on day 2 causes a dramatic revenue reduction as shown in Table IV. The generated scenarios cause the SOC approximation model to estimate the revenue poorly and produce unfavorable SOC headrooms. This indicates that LMP scenarios of low quality could lead to a cliff-like decline in revenue.

In addition, for PSH 2 with a maximum forecasting error of ±5% and PSH 1 with a maximum forecasting error of ±10%, they even have higher total revenues than the ideal setup, i.e., +$62.31 and +$0.21, as shown in Table V. This is also a result of the approximated revenue error. Intuitively, even the optimal SOC headrooms produced under the ideal setup cannot affirmatively lead to the best revenue from the actual market clearing. Thus, it is possible that with scenarios other than the ideal setup, the coincidentally produced SOC headrooms could lead to higher revenues.

E. Computational Performance of DE-based Algorithm

The computational performance of the DE-based algorithm in solving the proposed optimal SOC headroom model is further assessed. As discussed in Section III, with proper granularity, brute-force search could produce a near-optimal solution, which will be used as a benchmark to evaluate the solution quality of the DE-based algorithm. To avoid the excessive computational burden, the searching process is conducted via a two-round strategy: the first round uses a discretization granularity of 5 MWh, namely 5% of the capacity; and after it is done, the range of ±5 MWh around the best point identified in the first round will be explored in the second round with a refined discretization granularity of 1 MWh. The final best solution from the second round will be compared with the solution from the DE-based algorithm. We evaluate the performance of the DE-based algorithm via 10 cases that are composed of different DA and RT LMP scenarios for PSH 1. All 10 cases are solved with the same settings of $K=50$ (number of iterations), $N=20$ (population of points), $F=0.7$ (rescaling factor), and $R=0.9$ (crossing rate). These settings follow the recommendation in [21].

The proposed DE-based algorithm converges in 9 out of the 10 cases except case 8, showing that the settings are effective. Furthermore, in case 8, after 50 iterations, 3 points (out of 20) linger around a slightly worse solution, while the other 17 points converge to a better solution. The results are compared in Fig. 6. In all 10 cases, the objective values from the DE-based algorithm are no smaller than those from the brute-force search, indicating that the DE-based algorithm finds sub-optimal solutions that are better or at least close. In addition, except case 2, Euclidean distances of solutions from the DE-based algorithm and the brute-force search are all smaller than the maximum difference, i.e., $\sqrt{2}$, corresponding to the discretization granularity of 1 MWh, showing the solutions found by the two algorithms are rather close. Although case 2 presents the largest Euclidean distance, the objective values from the two algorithms are the same, suggesting that the two algorithms have derived different solutions with the same level of optimality.

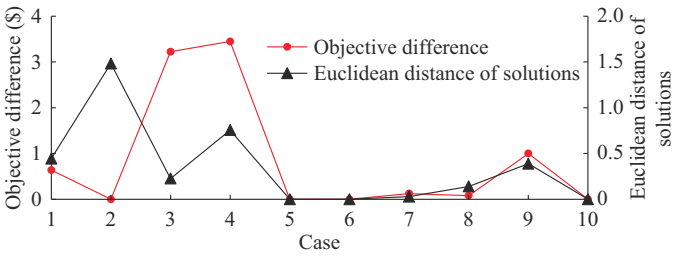

Fig. 6. Comparisons of proposed DE-based algorithm and brute-force search.

In fact, the optimal SOC headroom problem could have multiple optimal solutions due to the presence of power pumping and generating lower bounds of PSHs. With the power lower bounds, each switch of the operation mode, i.e., from idle to pumping and generating or from pumping and generating to idle, implicates a minimum change on SOC. Thus, at the DA scheduling level, when the changes of the SOC headroom are unable to accommodate the minimum SOC change induced by an additional PSH mode switch, the scheduling result of the DA scheduling level will no longer change. That is, there could exist multiple SOC headroom solutions corresponding to the same DA market results and consequently the same objective value (5), i.e., multiple optimal solutions may exist. The solution plane of case 2 with a granularity of 1 MWh is plotted in Fig. 7. It shows that flat planes appear in multiple areas of h^{L} and h^{U}, indicating solutions in these areas have the same objective values, i.e., revenues. Particularly, it can be observed that the flat plane in the area of h^{L}=[26, 30]MWh and h^{U}=[45, 50]MWh has the highest objective value, suggesting that there are multiple optimal solutions. It is worthwhile to mention that because the SOC headroom is a parameter submitted by the PSH to the RTO, rather than an operational instruction issued by the RTO to the PSH, the PSH can choose to use any one of the obtained solutions and its economic consequence will not be compromised.

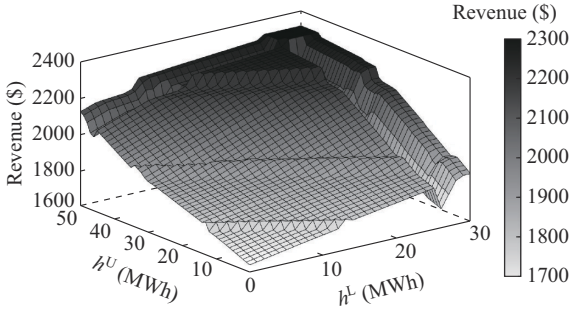

Fig. 7. Solution plane of case 2 with a granularity of 1 MWh.

It is worthwhile to mention that due to the repeated calculation of the DA and RT scheduling levels, the DE-based algorithm might face a considerable computational burden. As for these 10 cases, the average computational time is 1020 s. However, as part of the bidding preparation process that is done offline, the computational burden would be practically acceptable.

V. Conclusion

Following the idea of removing PSH bids from the objective functions of DA and RT markets of RTO as proposed in [6] and [18], this paper considers a future scenario that PSHs could be allowed to submit SOC headrooms in the DA market and discusses the possibility of increasing the total revenues of PSHs through optimizing such SOC headrooms. The proposed tri-level optimal SOC headroom model shows a strong ability to assist PSHs in determining the optimal SOC headrooms by properly mimicking how RTOs schedule their resources in the DA and RT markets. The DE-based algorithm can effectively solve the tri-level model and produce good-enough solutions with acceptable approximated revenue errors.

Case studies illustrate that SOC headrooms can help PSHs achieve higher revenues, while the magnitude of such increases depends on the LMP volatilities of the two markets. In some cases, the optimal SOC model may suggest zero SOC headrooms, indicating that there is no room for arbitrage based on the simulated DA and RT LMPs. The SOC headrooms and the associated profitability also strongly depend on the quality of simulated LMPs. Thus, compared to not submitting SOC headrooms, although there is a chance to achieve higher revenues, PSHs also bear financial risks of possible revenue loss, especially when LMP forecasting qualities are low. In our future work, we will consider reducing the sensitivity of profitability to LMP forecasting by constructing a closed-loop predict-and-optimize framework. In addition, ancillary services from PSHs will also be studied by leveraging the economics and security aspects of the headroom.

Appendix A

Similar to other evolutionary methods, first, a population of N points is randomly generated to initialize h_0^{Ln} and h_0^{Un} for $n = 1, 2, \ldots, N$. In each DE iteration k ($k = 1, 2, \ldots, K$), the DE-based algorithm first applies strategies such as rescaling and crossing and adds additional randomness on each point n ($n = 1, 2, \ldots, N$) to generate new tentative points. Then, with the tentative points, the DA scheduling level of RTO is solved and the solutions to $u_{\tau(v),s}^{G,DA}$ and $u_{\tau(v),s}^{P,DA}$ are passed to the RT scheduling level of RTO that will be solved next. The results from the two levels are used to assess the objective value of individual tentative points. For each point n, if its objective value is smaller than that of the corresponding tentative point, point n will be updated with its corresponding tentative point; otherwise, point n will keep unchanged. After all the points have been processed, the DE-based algorithm enters the next iteration. This iterative process terminates after a given number of interactions is reached. After the algorithm terminates, the point with the highest objective value is picked as the final solution. It is worth mentioning that during the iterative process, for an infeasible point, its corresponding objective value is set as negative infinity, and its values h^L and h^U violating [0, $H^{L,LIM}$] and [0, $H^{U,LIM}$] are fixed to the closest boundary.

The pseudocode of DE-based algorithm is shown in Appendix A Algorithm A1, where $\hat{h}^{Ln}$ and $\hat{h}^{Un}$ are the temporal values to h^L and h^U of point n; h_k^{Ln} and h_k^{Un} are the value to h^L and h^U of point n at iteration k; and $Rand(0, 1)$ is the random decimal between 0 and 1.

Algorithm 1: DE-based algorithm

Input: K, N, F, R

For $n = 1, 2, \ldots, N$

  Initialize $\langle h_k^{Ln}, h_k^{Un} \rangle$ and calculate its objective value

End for

For $k = 1, 2, \ldots, K$

  For $n = 1, 2, \ldots, N$

    Randomly select three district points from all points other than point n: $\langle h_k^{Ln1}, h_k^{Un1} \rangle$, $\langle h_k^{Ln2}, h_k^{Un2} \rangle$, $\langle h_k^{Ln3}, h_k^{Un3} \rangle$

    Randomly select an element in h^L and h^U

    If h^L is selected

      $\hat{h}^{Ln} = h_k^{Ln} + F\left(h_k^{Ln3} - h_k^{Ln}\right) + F\left(h_k^{Ln1} - h_k^{Ln2}\right)$

      If $Rand(0, 1) \le R$

        $\hat{h}^{Un} = h_k^{Un} + F\left(h_k^{Un3} - h_k^{Un}\right) + F\left(h_k^{Un1} - h_k^{Un2}\right)$

      Else

        $\hat{h}^{Un} = h_k^{Un}$

      End if

    Else /* h^U must have been selected */

      $\hat{h}^{Un} = h_k^{Un} + F\left(h_k^{Un3} - h_k^{Un}\right) + F\left(h_k^{Un1} - h_k^{Un2}\right)$

      If $Rand(0, 1) \le R$

        $\hat{h}^{Ln} = h_k^{Ln} + F\left(h_k^{Ln3} - h_k^{Ln}\right) + F\left(h_k^{Ln1} - h_k^{Ln2}\right)$

      Else

        $\hat{h}^{Ln} = h_k^{Ln}$

      End if

    End if

    Set $\hat{h}^{Ln} = \min\left\{\max\left\{0, \hat{h}^{Ln}\right\}, H^{L,LIM}\right\}$ and $\hat{h}^{Un} = \min\left\{\max\left\{0, \hat{h}^{Un}\right\}, H^{U,LIM}\right\}$

    Solve the DA scheduling level of RTO with $\langle \hat{h}^{Ln}, \hat{h}^{U} \rangle$

    Solve the RT scheduling level of RTO with the solution of the DA market level

    Calculate objective value with the solutions from DA and RT markets

    If objective value with $\langle \hat{h}^{Ln}, \hat{h}^{Un} \rangle$ is not smaller than the objective value with $\langle h_k^{Ln}, h_k^{Un} \rangle$

      $\langle h_k^{Ln}, h_k^{Un} \rangle = \langle \hat{h}^{Ln}, \hat{h}^{Un} \rangle$; $\langle h_{k+1}^{Ln}, h_{k+1}^{Un} \rangle = \langle \hat{h}^{Ln}, \hat{h}^{Un} \rangle$

    Else

      $\langle h_{k+1}^{Ln}, h_{k+1}^{Un} \rangle = \langle h_k^{Ln}, h_k^{Un} \rangle$

    End if

  End for

End for

References

[1] MISO. (2021, Jun.). 2020 state of the market report for the MISO electricity markets. [Online]. Available: https://www. potomaceconomics. com/wp-content/uploads/2021/05/2020-MISO-SOM_Report_Body_Compiled_Final_rev-6-1-21.pdf

[2] P. Ilak, I. Kuzle, L. Herenčić *et al*., "Market power of coordinated hydro-wind joint bidding: croatian power system case study," *Journal of Modern Power Systems and Clean Energy*, vol. 10, no. 2, pp. 531-541, Mar. 2022.

[3] C. Dai, Y. Chen, F. Wang *et al*., "A configuration-component-based hybrid model for combined-cycle units in MISO day-ahead market," *IEEE Transactions on Power Systems*, vol. 34, no. 2, pp. 883-896, Mar. 2019.

[4] Y. Liu, L. Wu, J. Li *et al*., "Towards accurate modeling on configuration transitions and dynamic ramping of combined-cycle units in UC problems," *IEEE Transactions on Power Systems*, vol. 35, no. 3, pp. 2200-2211, May 2020.

[5] R. Jiang, J. Wang, and Y. Guan, "Robust unit commitment with wind power and pumped storage hydro," *IEEE Transactions on Power Systems*, vol. 27, no. 2, pp. 800-810, May 2012.
[6] B. Huang, Y. Chen, and R. Baldick, "A configuration based pumped storage hydro model in the MISO day-ahead market," *IEEE Transactions on Power Systems*, vol. 37, no. 1, pp. 132-141, Jan. 2022.
[7] M. A. Hozouri, A. Abbaspour, M. Fotuhi-Firuzabad *et al*., "On the use of pumped storage for wind energy maximization in transmission-constrained power systems," *IEEE Transactions on Power Systems*, vol. 30, no. 2, pp. 1017-1025, Mar. 2015.
[8] J. García-González, R. M. R. Muela, L. M. Santos *et al*., "Stochastic joint optimization of wind generation and pumped-storage units in an electricity market," *IEEE Transactions on Power Systems*, vol. 23, no. 2, pp. 460-467, May 2008.
[9] A. Golshani, W. Sun, Q. Zhou *et al*., "Coordination of wind farm and pumped-storage hydro for a self-healing power grid," *IEEE Transactions on Sustainable Energy*, vol. 9, no. 4, pp. 1910-1920, Oct. 2018.
[10] M. E. Khodayar, M. Shahidehpour, and L. Wu, "Enhancing the dispatchability of variable wind generation by coordination with pumped-storage hydro units in stochastic power systems," *IEEE Transactions on Power Systems*, vol. 28, no. 3, pp. 2808-2818, Aug. 2013.
[11] S. Wang, J. Liu, H. Chen *et al*., "Modeling state transition and head-dependent efficiency curve for pumped storage hydro in look-ahead dispatch," *IEEE Transactions on Power Systems*, vol. 36, no. 6, pp. 5396-5407, Nov. 2021.
[12] T. Ma, H. Yang, L. Lu *et al*., "Pumped storage-based standalone photovoltaic power generation system: modeling and techno-economic optimization," *Applied Energy*, vol. 137, no. 1, pp. 649-659, Jan. 2015.
[13] Z. Zhao, C. Cheng, S. Liao *et al*., "A MILP based framework for the hydro unit commitment considering irregular forbidden zone related constraints," *IEEE Transactions on Power Systems*, vol. 36, no. 3, pp. 1819-1832, May 2020.
[14] K. Bruninx, Y. Dvorkin, E. Delarue *et al*., "Coupling pumped hydro energy storage with unit commitment," *IEEE Transactions on Sustainable Energy*, vol. 7, no. 2, pp. 786-796, Apr. 2016.
[15] N. Li and K.W. Hedman, "Enhanced pumped hydro storage utilization using policy functions," *IEEE Transactions on Power Systems*, vol. 32, no. 2, pp. 1089-1102, May 2017.
[16] Z. Tang, Y. Liu, and L. Wu, "Reserve model of energy storage in day-ahead joint energy and reserve markets: a stochastic UC solution," *IEEE Transactions on Smart Grid*, vol. 12, no. 1, pp. 372-382, Jan. 2021.
[17] Y. Liu, Z. Tang, and L. Wu, "On secured spinning reserve deployment of energy-limited resources against contingencies," *IEEE Transactions on Power Systems*, vol. 37, no. 1, pp. 518-529, Jan. 2022.
[18] B. Huang, A. Ghesmati, Y. Chen *et al*. (2021, Jan.). Pumped storage optimization in day-ahead and real-time market under uncertainty. [Online]. Available: https://www.ferc.gov/media/t2-huang.
[19] D. A. Schiro, T. Zheng, F. Zhao *et al*., "Convex hull pricing in electricity markets: formulation, analysis, and implementation challenges," *IEEE Transactions on Power Systems*, vol. 31, no. 5, pp. 4068-4075, Sept. 2016.
[20] A. Ghesmati, B. Huang, Y. Chen *et al*., "Probabilistic real-time price forecast and the application to pumped storage hydro unit optimization," in *Proceedings of 2022 IEEE PES General Meeting*, Denver, USA, Jul. 2022, pp. 1-8.
[21] J. S. Angelo, E. Krempser, and H. J. C Barbosa, "Differential evolution for bilevel programming," in *Proceedings of 2013 IEEE Evolutionary Computation Congress*, Cancun, Mexico, Jun. 2013, pp. 470-477.
[22] Y. Lin, B, Huang, Y. Lin *et al*. (2023, Jan.). PSH testing data and DE pseudocode. [Online]. Available: https://drive. google. com/file/d/1TGrzMp0cysaUlhO_Gfi8bMQ-SxXl6UuA/view?usp=sharing.
[23] NYISO. (2022, Jun.) Transmission and dispatch operations manual. [Online]. Available: https://www.nyiso.com/manuals-tech-bulletins-user-guides.

Yikui Liu received the B.S. degree in electrical engineering and automation from Nanjing Institute of Technology, Nanjing, China, in 2012, the M.S. degree in power system and automation from Sichuan University, Chengdu, China, in 2015, and the Ph.D. degree in electrical and computer engineering from Stevens Institute of Technology, Hoboken, USA, in 2020. He worked in Siemens, USA, as an Energy Market Engineer, from 2020 to 2021. He was a Postdoctoral in Stevens Institute of Technology, Hoboken, USA, from 2021 to 2023. His research interests include energy market and energy economics.

Bing Huang received the B.E. degree in electrical engineering from North China Electric Power University, Baoding, China, in 2012, the M.S. degree in electrical engineering from George Washington University, Washington DC, USA, in 2014, and the Ph.D. degree in electrical engineering from The University of Texas at Austin, Austin, USA, in 2019. He is currently an R&D Research Engineer with the Midcontinent Independent System Operator, Inc., Carmel, USA. His research interests include stochastic programming and its application.

Yang Lin received the B.S degree in mathematics, information and computational sciences from Xiamen University, Xiamen, China, in 2011, the M.S. degree in mathematics from New York University, New York, USA, in 2014, and the Ph.D. degree in applied mathematics from Stevens Institute of Technology, Hoboken, USA, 2020. He was a Postdoctoral in Stevens Institute of Technology, from 2020 to 2021. Currently, he is a Research Scientist in Munich Re/HSB. His research interests include stochastic programming and its application.

Yonghong Chen received the B. S. degree in electrical engineering from Southeast University, Nanjing, China, the M.S. degree in electrical engineering from Nanjing Automation Research Institute, Nanjing, China, the Ph.D. degree in electrical engineering from Washington State University, Pullman, USA, and the M.B.A. degree from the Kelly School of Business, Indiana University, Indianapolis, USA. She is currently a Consulting Advisor with Midcontinent Independent System Operator (MISO). Her research interests include research and development to address challenges on market design and market clearing system.

Lei Wu received the B.S. degree in electrical engineering and the M.S. degree in systems engineering from Xi'an Jiaotong University, Xi'an, China, in 2001 and 2004, respectively, and the Ph.D. degree in electrical engineering from the Illinois Institute of Technology, Chicago, USA, in 2008. From 2008 to 2010, he was a Senior Research Associate with the Robert W. Galvin Center for Electricity Innovation. In 2012, he was a summer Visiting Faculty with New York Independent System Operator (NYISO). He was a Professor with Electrical and Computer Engineering Department, Clarkson University, Potsdam, USA, till 2018. He is currently the Anson Wood Burchard Chair Professor with the Electrical and Computer Engineering Department, Stevens Institute of Technology, Hoboken, USA. His research interests include power system operation and planning, energy economics, and community resilience microgrid.